SSIM 2025 - JJ Potter & J Wesseloo (eds)

doi:10.36487/ACG_repo/2535_34

3D block stability analysis of rock slope in Pilbara iron ore operations

Isaac Ahenkorah [a,*], Samantha Hinks [a], Adam Cooper [a]

[a] *Rio Tinto, Australia*

Abstract

The lithostratigraphic conditions in the Pilbara region of Western Australia are characterised by complex structural features resulting from multiple deformation events leading to significant folding, faulting, jointing/discontinuities, and unfavourable bedding orientations. These complexities present challenges in open pit iron ore mining as they can trigger slope instabilities with considerable safety and economic implications. Improved confidence in stability assessments of large rock slopes can be achieved through a better understanding of the persistence, distribution, and location of unstable blocks within the slope, utilising true 3D geometry. This paper examines the 3D block stability of a planar sliding failure in an open pit iron ore mine using Rocscience RocSlope3. Joints measured via an unmanned aerial vehicle photogrammetry mapping campaign (verified with in-field mapping data) were modelled as planar surfaces, incorporating their orientation, location, and properties (shear strength, persistence and waviness). The limit equilibrium method was applied to assess the stability of each block, predict potential failure locations and magnitudes, and generate heat maps indicating areas with the lowest Factors of Safety, largest failure volumes, and greatest depths. The results demonstrated that valid unstable blocks were formed by intersecting discontinuities, with failure initiated by daylighting and the detachment of blocks. The predicted location and volume of failed blocks, with a Factor of Safety below 1.0, aligned with bench crest failures observed in the field. Overall, the 3D block stability analysis method using Rocscience RocSlope3 offers a promising approach for identifying potential bench crest failures, multi-bench failures, and conducting global slope risk assessments in open pit rock slopes.

Keywords: *open pit, slope instability, block stability, kinematic analysis*

1 Introduction

Geological discontinuities such as beddings, faults, joints, and fractures play a dominant role in rock mass failure compared to intact rock (Dixon et al. 2011). Rock mass strength within the Pilbara iron ore region is strongly anisotropic, with weak shale beds inter-bedded with strong banded iron formations (BIFs). Individual bedding surfaces are highly persistent and well defined across the Pilbara with banding down to the centimetre scale being traceable over hundreds of kilometres (Trendall & Blockley 1970; Dixon et al. 2011). The dominant instability mechanism in this region is structurally controlled planar sliding on adversely oriented primary bedding surfaces often interacting with large-scale structures (e.g. bedding, faults, joints and/or dykes) providing side release or complex slip surface geometries. At the mine scale, the persistence of bedding is essentially infinite, leading to potential structurally controlled instabilities. These instabilities are prominent in areas where the bedding dips at an unfavourable angle out of the slope and greater than the angle of friction of the discontinuity surface (Bonilla-Sierra et al. 2017; Mensah et al. 2025).

Understanding the influence of structural discontinuities and unexpected variations in bedding shear strength on the stability of slopes is therefore an integral part of Pilbara slope design. Historically, the risks associated with slope instability have been analysed using 2D and 3D limit equilibrium methods (LEM) and

* Corresponding author. Email address: isaac.ahenkorah@riotinto.com

other numerical methods. However, the interaction between individual blocks separated by the discontinuities is usually not considered in LEM (Sun et al. 2011). To address this issue, kinematic analysis using simple methods (e.g. Dips, SWedge, RocPlane and RocTopple) have been adopted in past studies to assess the stability of rock slopes with structures represented as explicit discontinuities (Khanna & Dubey 2021; Pradhan & Siddique 2020; Bekele & Meten 2023; Mensah et al. 2025). Although these existing methods have been industry staples for years, allowing users to effectively analyse various failure mechanisms, there is a need for large-scale rock slope analysis in both the civil and mining industries. This study, therefore, investigates 3D block stability analysis in rock slopes susceptible to structurally controlled failures using Rocscience RocSlope3 software version 1.007 (Rocscience Inc 2023). The key focus of this study is to assess existing bench crest failure in an open pit slope using structure sets (bedding planes and joints) measured via an unmanned aerial vehicle photogrammetry mapping campaign.

The methodology employed in this study enables the identification of bench crest failures, multi-bench (inter-ramp) crest failures, and comprehensive global slope risk assessments. By incorporating true 3D slope geometry, the analysis can capture key blocks formed by the intersection of geological structures such as faults, joints, and bedding planes. This provides valuable insights into the size and probability of translational block failures across different slope regions. Additionally, this method facilitates the following capabilities:

- identification of intersecting and persistent discontinuities that form discrete, daylighting blocks with potential for detachment
- calculation of block Factors of Safety (FoS) by simulating the effects of various forces, including seismic activity, external loading, water pressure, ground support, and joint shear strength
- localisation of slope areas with the lowest FoS, largest potential failure volumes, and highest support requirements
- execution of probabilistic analyses to quantify failure risks.

It is particularly important to recognise that key blocks, which are critical to potential failure, only form when multiple joints intersect in such a way that they enclose a finite volume and extend persistently enough to detach from the surrounding rock mass (Figure 1). The simulation of such intersecting joints allows RocSlope3 to model removable blocks that daylight (i.e. emerge) on the slope face. These removable blocks are key contributors to structurally controlled slope failures. Furthermore, RocSlope3 has the capability to simulate progressive block failure, where the detachment of one block can destabilise adjacent blocks, leading to a cascading failure mechanism.

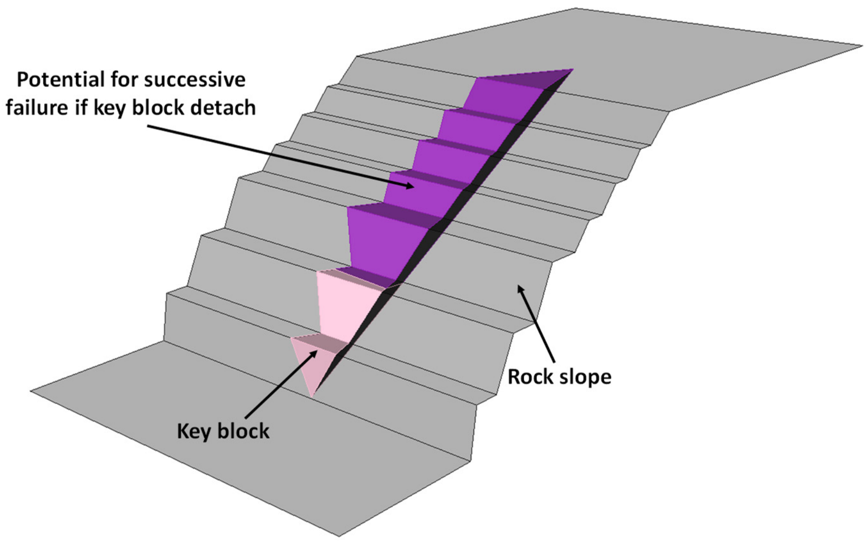

Figure 1 Overview of three-dimensional block stability analysis from RocSlope3

2 Local geology and structural complexity

The Pilbara region of Western Australia is widely known for its enormous deposits of high-quality iron ore, positioning it as one of the world's most significant iron ore mining locations. Nonetheless, iron ore mining in this region poses its own set of geotechnical issues, characterised by ancient, weathered rock formations that are frequently unstable. These formations are related to the occurrence of iron ore deposits, which originated from ancient BIFs produced over billions of years. The intricate characteristics of these geological formations such as folding, faulting, and shearing, present substantial hurdles to mining operations (Dixon et al. 2011).

Past studies have indicated that slope instability in most hard rock Pilbara iron ore operations is predominantly controlled by structural mechanisms (Dixon et al. 2011; Goldstein et al. 2023). As open pit mining extends deeper with steeper slopes in complex geological formations, the frequency and severity of slope failures would potentially increase. Goldstein et al. (2023) assessed 144 documented failed slope cases (41 cases are of multi-batter and 103 are cases of single batter fall of grounds) from more than a dozen open pit iron ore mines in Australia. The results from their study indicated that about 70% of the failed slopes were caused by planar sliding on adversely oriented primary bedding surfaces. A typical example of structurally controlled slope failures within open pit iron ore mines in the Pilbara region of Western Australia are shown in Figure 2.

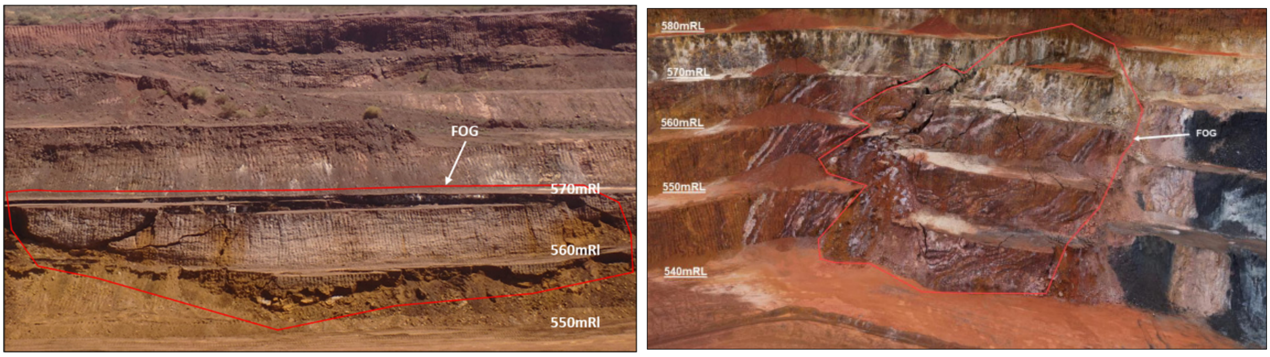

(a) (b)

Figure 2 Examples of instability along bedding planes in open pit iron ore mines in the Pilbara region. (a) Planar sliding failure along a shale band; (b) Wedge failure along a shale band contact and a Fault plane

3 Assessment of structural controlled failure: case example

The following structurally controlled slope example in an open pit iron ore mining was used to assess the effectiveness of the recently introduced Rocscience RocSlope3 software version 1.007 (Rocscience Inc 2023). This pit example represents a single batter crest failure (between the 640 and 630mRl), which occurred on the southern section of the pit. The dominating failure mechanism in this pit is mostly planar and wedge sliding along major shale bands and joint planes. The bedding in this pit area has a shallower angle (average of ~47°), daylighting into the batter face of the design slope (65°). During slope excavation, the batters are often pulled along the bedding planes resulting in a non-conformance between the design and pre-failure as-built better face angle (65 versus 47°) and berm width (8 versus 5 m). A representative cross-section taken through the study area is shown in Figure 3 below.

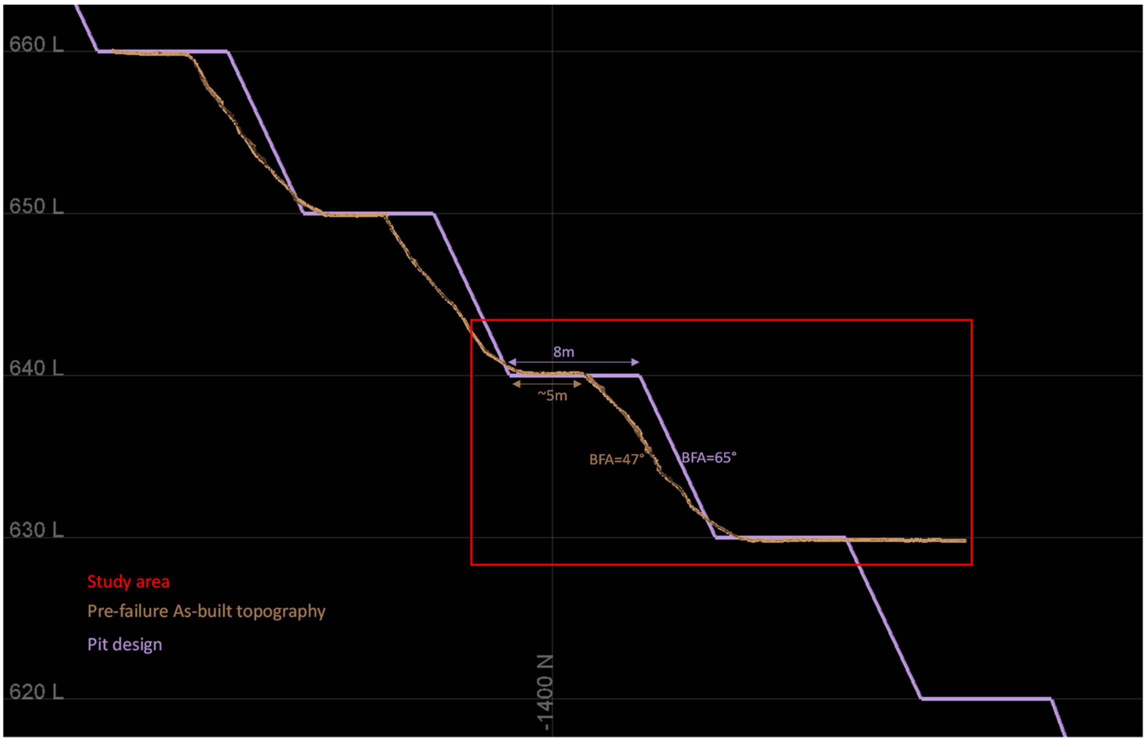

Figure 3 Cross-section through study area indicating poor design conformance

The slope failure was estimated to extend approximately 28 m horizontally along the face, penetrate 1.5 m into the batter face, and about 4 m in height from the crest. The run-out distance of blocky material from the as-built toe of the slope was approximately 2 m. By overlaying the triangulations of the pre-failure and post-failure surfaces, the failure volume was estimated to be of around 84 m^3. The weight of the dislodged material was estimated at approximately 240 t using a unit weight of 28 kN/m^3. The fall height of the material from the failure crest to its final resting position at the toe was about 10 m, indicating significant potential for energy release and impact at the base. The failure appears to be structurally controlled, with geological discontinuities, particularly undercut bedding planes and joint sets, playing a key role in the detachment and movement of the rock mass. Field evidence of these structural features, as well as the dimensions and morphology of the failure surface (or 'failure scalp'), is shown in Figures 4 and 5 below.

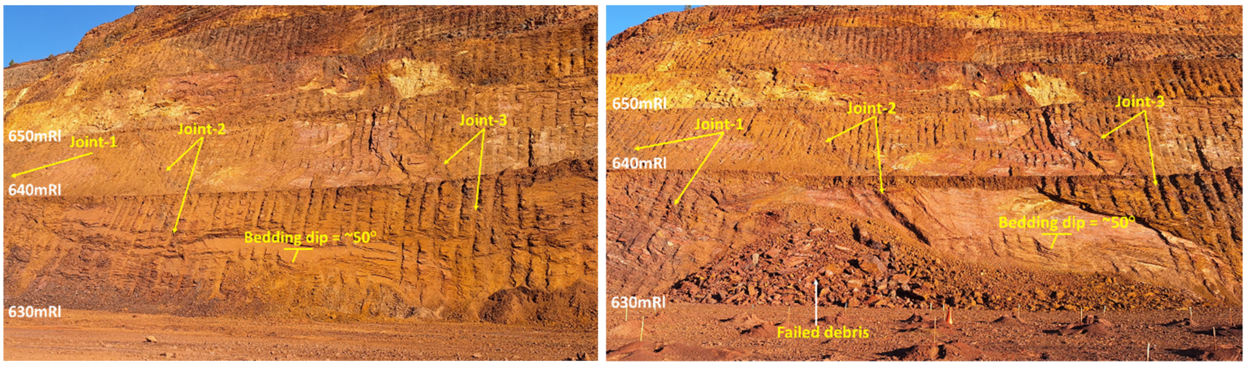

(a) (b)

Figure 4 Overview of single batter crest failures in structurally controlled pit slopes. (a) Pit slope with undercut bedding planes and joints in May 2024; (b) Pit slope with failure in June 2024

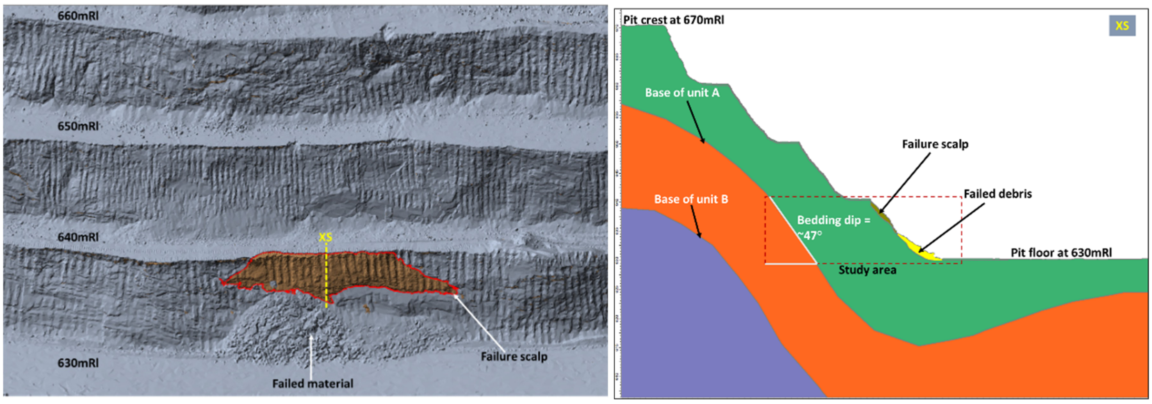

(a) (b)

Figure 5 Overview of a single batter crest failure in a structurally controlled pit slope. (a) 3D view looking south; (b) 2D geological cross-section through failure

3.1 Mapping data and methods

3.1.1 Drone photogrammetry

A 3D point cloud was generated by taking overlapping aerial images captured using a DJI Mavic 3 drone equipped with a 20 MP camera. The flightpath consisted of flying the drone 5 to 15 m from the slope face for four passes with varying camera inclinations as outlined below:

- overview pass with the camera angled at ~20–45°
- front on pass with the camera angled at 0°
- close-up pass with the camera angled at 0°
- low pass with camera looking up at 20°.

In total, 136 overlapping images were taken to generate the points cloud. The points cloud was generated using Bentley Systems ContextCapture software with the Spatial Reference System set to WGS 84 / UTM zone 50S (Figure 6). The point cloud was then opened in CloudCompare, a free open-source point cloud processing and editing tool, and the Compass plugin was used to measure the orientation of discontinuity planes. A sense check was carried out on the data by comparing it to previous hand mapping data collected for the same area. A total of 18 discontinuities were identified for use in this study.

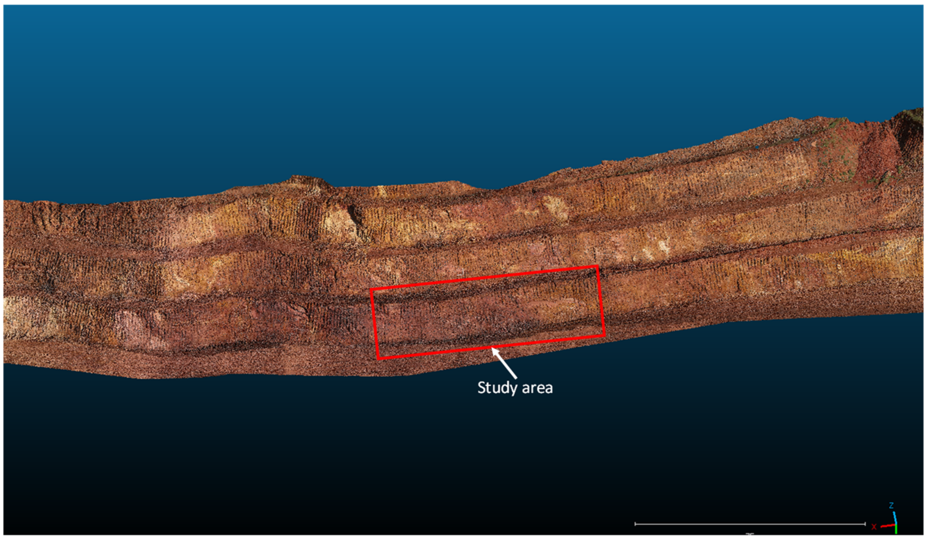

Figure 6 Point cloud with area of interest indicated by the red box

3.2 Kinematic analysis

A total of 18 mapped discontinuities were obtained through drone photogrammetry for use in the analysis, the data is outlined in Table 1. Bedding (BG) and joint set planes (JN) have been generated using Rocscience Dips software version 8.029 (Rocscience Inc 2004) as shown in Figure 7. The design slope and pre-failure as-built slope parameters, along with the discontinuity strength parameters, are presented in Table 2.

Table 1 Discontinuity orientation data

Dip (°)	Dip direction (°)	X (m)	Y (m)	Z (m)	Discontinuity type
52	350	11,207	−1,394	635	Bedding plane (BG)
50	345	11,206	−1,394	634	BG
52	356	11,198	−1,396	634	BG
49	358	11,196	−1,395	634	BG
59	359	11,222	−1,395	637	BG
44	353	11,203	−1,395	635	BG
53	359	11,196	−1,394	633	BG
54	360	11,193	−1,394	634	BG
41	357	11,196	−1,396	637	BG
40	349	11,209	−1,396	638	BG
39	359	11,210	−1,398	640	BG
38	344	11,211	−1,397	639	BG
39	354	11,204	−1,397	636	BG
57	351	11,228	−1,393	635	BG
37	359	11,202	−1,395	633	BG
72	242	11,211	−1,394	634	Joint set plane (JN)
73	241	11,184	−1,395	635	JN
68	240	11,228	−1,392	635	JN

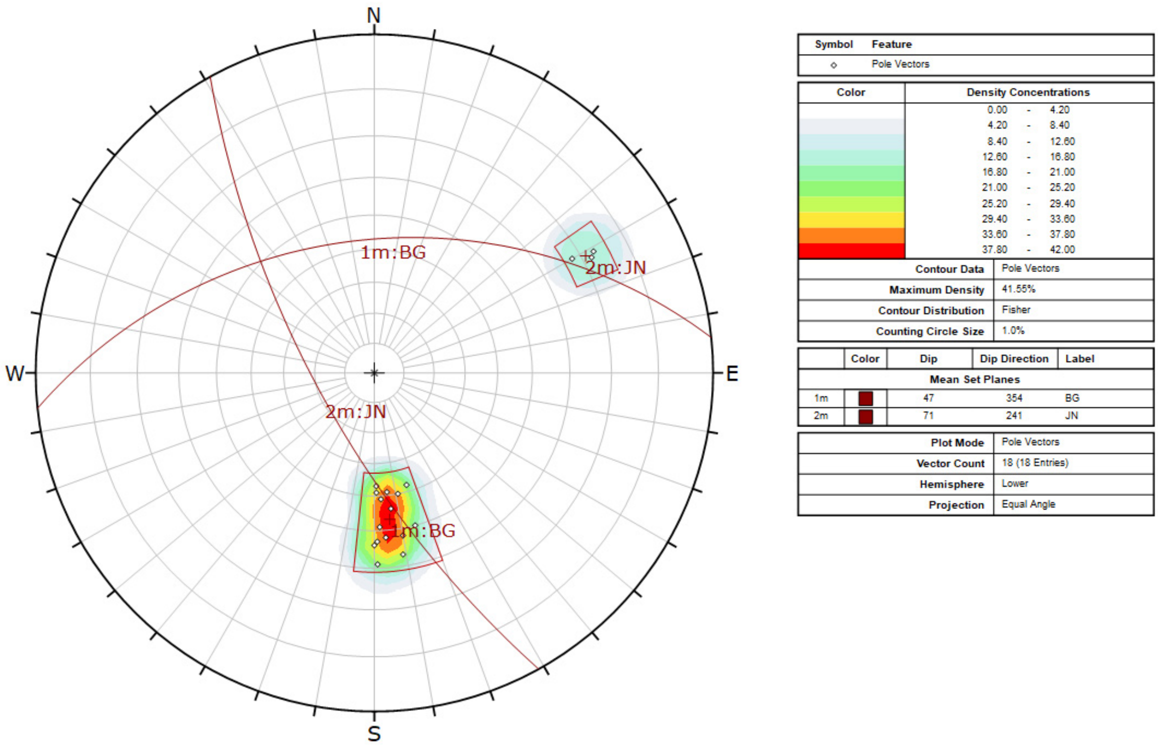

Figure 7 Dips analysis of discontinuity data

Table 2 Pit design and pre-failure as-built slope data

Properties	Pit design	Pre-failure as-built
Slope dip (°)	65	47
Slope dip direction (°)	354	353
Slope width (m)	8	5
Slope height (m)	10	10
Friction angle (°)	37	37

The results from the kinematic analysis are presented in Table 3 below. The results indicate that 100% of bedding plane poles fall within the critical zone for planar failure for pit design parameters, in comparison to 46.7% for pre-failure as-built parameters (Figures 8). The analysis also indicates that 79.1% of intersections between BG and JN within the critical zone for wedge sliding failure for pit design parameters, in comparison to 40.5% for pre-failure as-built parameters (Figures 9).

The mean BG orientation recorded during this study has a dip of 47°, which is the same as the bench face angle of the pre-failure as-built slope. This is likely due to operational decisions to scale the slope face back to the BG, to reduce the risk of structural failure. Kinematic analysis indicates that scaling the batter face back to 47° results in a 53.3% reduction in the failure percentage for planar failures and a 38.6% reduction for wedge failures. However, this adjustment does not eliminate the potential for these failure modes entirely, as some discontinuities still have the potential to daylight into the slope face.

Although Dips analysis is an effective method for determining potential failure modes, it does not account for the dimensions of the failure blocks. Additional analysis in RocSlope3 is required to further understand the failure mechanisms and potential failure block sizes.

Table 3 Kinematic analysis results

Kinematic analysis type	Failure percentage (%)	
	Pit design	Pre-failure as-built
Planar sliding (bedding plane [BG])	100.0	46.7
Wedge sliding (BG and joint set plane)	79.1	40.5

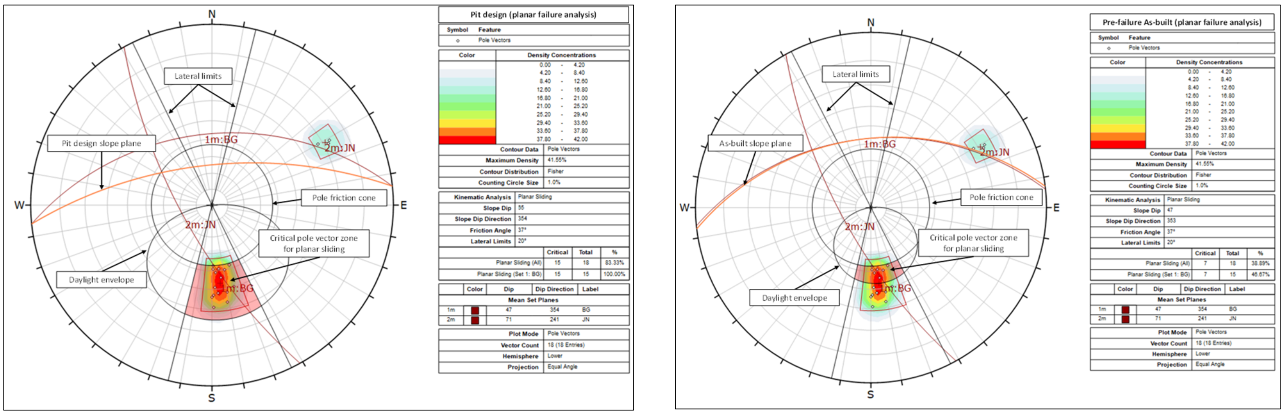

(a) (b)

Figure 8 Kinematic analysis: planar failure. (a) Pit design parameters; (b) Pre-failure as-built parameters

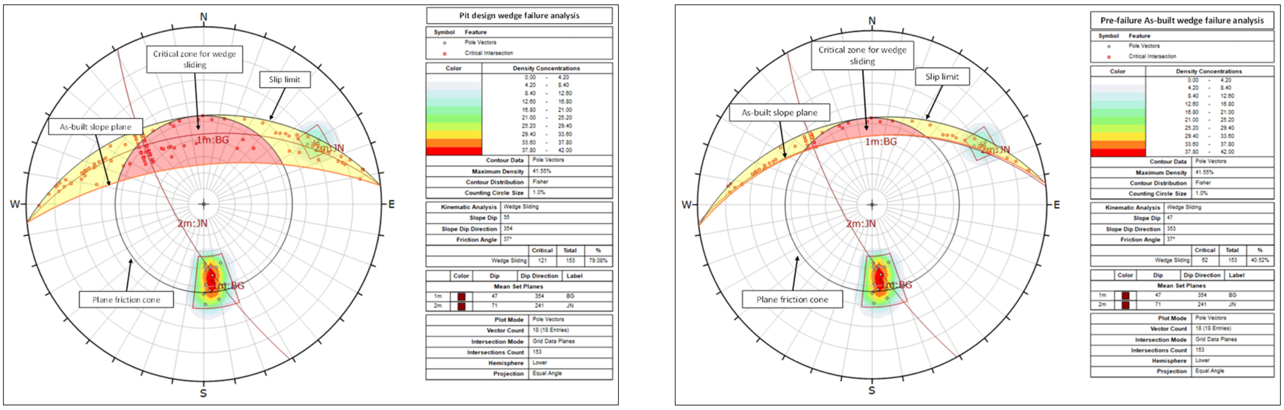

(a) (b)

Figure 9 Kinematic analysis: wedge failure. (a) Pit design parameters; (b) Pre-failure as-built parameters

3.3 3D block analysis

A 3D slope stability analysis was carried out using Rocscience RocSlope3 software version 1.007 (Rocscience Inc 2023) to assess structurally controlled failure mechanisms in rock slopes. A fundamental aspect of developing a representative and robust RocSlope3 model is the accurate definition of discrete, finite discontinuity surfaces. These surfaces are represented as planar features, with their definition requiring careful consideration of both geometric and mechanical attributes. Geometric parameters include persistence, defined by the orientation (dip and dip direction), spatial position, and extent (size) of each joint. Mechanical parameters include shear strength, surface waviness, and hydraulic conditions, specifically the influence of porewater pressure along the discontinuity planes. For this analysis, orientation data from 18 mapped discontinuities were used as input, as detailed in Table 1. These discontinuities were incorporated into the model using the 'defined measured joints' functionality within RocSlope3. Joint strength properties were defined using the Mohr–Coulomb failure criterion, with strength parameters derived from mean batter-scale shear strength test data corresponding to each discontinuity surface. To account for potential disturbance due to blasting activities, cohesion was conservatively set to 0 kPa for all discontinuities. Additionally, for model simplification, joint waviness was assumed to be 0°, representing planar surfaces. The model was considered under dry conditions, as the groundwater table was confirmed to be below the elevation of the current pit slope; therefore, no water pressure was applied along the discontinuities. A summary of the mechanical and geometric parameters assigned to each discontinuity set is provided in Table 4.

Table 4 Properties for all discontinuities

Properties	Bedding plane	Joint set plane
Cohesion (kPa)	0	0
Friction angle (°)	37	35
Unit weight (kN/m^3)	28	28
Waviness (°)	0	0
Water pressure method	Dry	Dry

Figure 10a displays a 3D representation of the slope with BG and JN visualised as discs. These discs represent the modelled planar features within the rock mass, highlighting their orientation, location, and spatial extent, providing understanding of how geological structures are input into the model. Figure 10b presents the joint trace patterns and the resulting valid key blocks that form where the joints intersect. These blocks meet the criteria for potential removal, and their geometry suggests susceptibility to failure. The visualisation supports interpretation of failure mechanisms by showing how complex joint networks interact to form defined, unstable volumes within the slope.

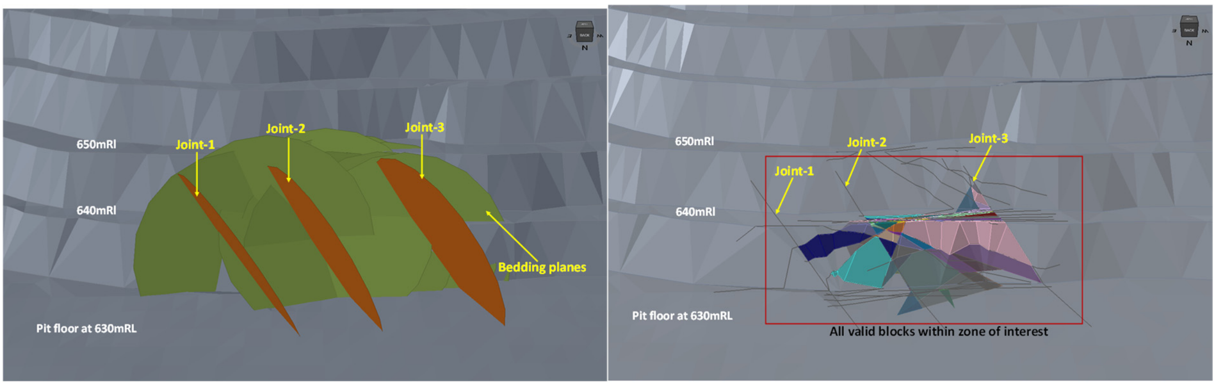

(a) (b)

Figure 10 Overview of 3D block slope from RocSlope3. (a) Bedding and joint discs; (b) Joint traces and the resulting valid blocks that form

3.3.1 Comparison of design and as-built slope

The 3D block stability analyses conducted for both the pit design and the pre-failure as-built slopes provide valuable insight into the influence of slope geometry on structurally controlled failure mechanisms. Both analyses were carried out using successive failure analysis within RocSlope3, based on a design FoS threshold of 1.0. In this approach, blocks with calculated FoS values less than 1.0 were classified as unstable and failed, while those with FoS values equal to or greater than 1.0 were considered stable. This method enables simulation of progressive failure mechanisms by removing unstable blocks and updating the model geometry and block interactions iteratively. A comparative assessment of the results reveals that the pit design slope exhibited a greater volume of failed material (~450 m^3) relative to the as-built slope (~82 m^3), highlighting the sensitivity of slope stability to batter angle and its interaction with geological structures (see Figures 11 and 12).

The batter face angle for the design slope was 65°, which is significantly steeper than the 47° batter angle measured in the as-built slope condition prior to failure. This steeper configuration resulted in a greater proportion of joint-defined blocks meeting the geometric criteria for removability and daylighting, particularly those aligned with dominant structural discontinuities. The mean dip of the mapped discontinuities was 47° (see Figure 7), effectively subparallel to the as-built slope face, which contributed to a relatively stable block geometry under those conditions. In contrast, the steeper 65° design batter cut across these discontinuities at a more unfavourable angle, increasing the exposure of persistent joint sets and enabling the formation of larger and more kinematically viable failure blocks. This was clearly reflected in the results from the kinematic analysis in Dips, which predicted a higher probability of failure in the design slope scenario.

These findings underscore the importance of ensuring that slope design geometry is compatible with local structural conditions. While steeper designs may be driven by economic considerations such as ore recovery and reduced stripping ratios, they can significantly compromise slope stability where adverse structural orientations are present. The alignment between the discontinuity dip angle (47°) and the as-built slope angle effectively reduced the driving forces acting on potential failure blocks, thereby enhancing overall stability.

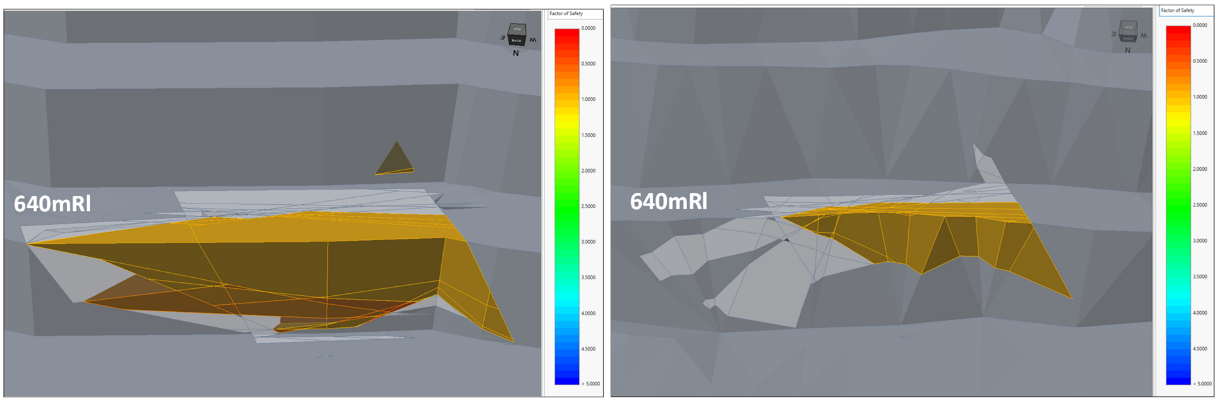

(a) (b)

Figure 11 Results of block slope stability analysis from RocSlope3 showing failed blocks with FoS < 1.0 in orange on the (a) pit design and (b) pre-failure as-built

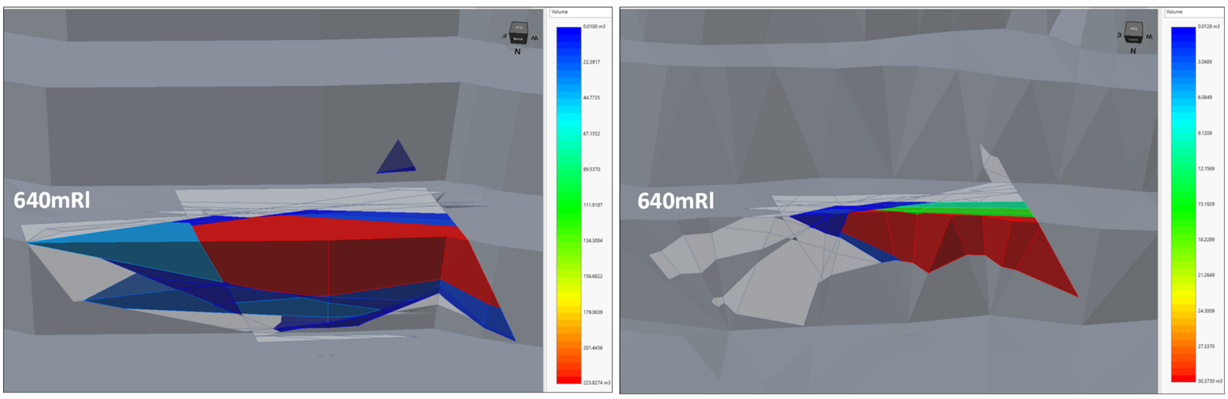

(a) (b)

Figure 12 Results of block slope stability analysis from RocSlope3 showing volume of failed blocks on the (a) pit design and (b) pre-failure as-built

3.3.2 Successive and non-successive failure

A comparative analysis was undertaken to evaluate the influence of the failure modelling methodology, specifically successive failure versus non-successive failure, on the prediction of structurally controlled slope instabilities using RocSlope3. The analyses were performed under identical geometrical conditions, with the only variable being the failure simulation approach (see Figure 13). In the non-successive failure analysis, the model identifies blocks that are kinematically removable based solely on their geometry, joint intersections, and limit equilibrium assessment, assuming the surrounding slope remains fully intact. This static approach assesses each block in isolation and does not consider the destabilising effects of adjacent block failures. As a result, the method tends to underestimate the extent and depth of potential failure, especially in structurally complex slopes where progressive failure mechanisms are expected. Conversely, the successive failure analysis simulates progressive failure by iteratively removing blocks with FoS less than 1.0, updating the slope geometry and block interactions after each iteration. This approach captures the cascading nature of structurally controlled failures, where the removal of one block reduces confinement and support to surrounding blocks, thereby triggering additional failures. The analysis, therefore, accounts for block interdependency and release surfaces that may not be evident in an initial static condition.

The results from the successive failure model indicate a significantly larger volume of failed material compared to the non-successive model. This increase is primarily due to the mobilisation of key blocks (discrete volumes of rock bounded by intersecting discontinuities) that become kinematically viable once support from neighbouring blocks is lost. In the non-successive analysis, many of these blocks remain artificially stable due to unchanging boundary conditions. Importantly, the volume and extent of failed material predicted in the successive failure analysis (~82 m^3) closely aligns with field observations of the actual slope failure (~84 m^3), indicating that the progressive block failure mechanism simulated in the model represents the dominant mode of slope collapse. In contrast, the non-successive model underestimates the failed volume (~30 m^3) and fails to capture the full extent of instability evident in the field. These findings demonstrate that successive failure modelling offers a more realistic and reliable representation of slope behaviour in structurally controlled rock masses. While the non-successive approach may be useful for preliminary assessments, it lacks the capacity to simulate the dynamic failure progression often observed in steep, jointed slopes. The results support the broader geotechnical practice of incorporating progressive failure methods in critical slope design, particularly in high-risk or structurally complex settings.

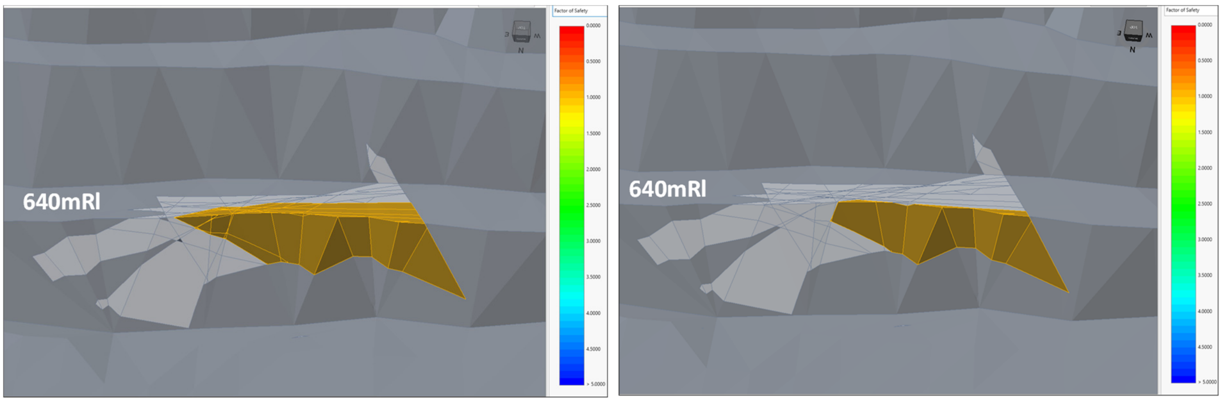

(a) (b)

Figure 13 Results of block slope stability analysis from RocSlope3 showing failed blocks with FoS < 1.0. (a) Successive failure analysis; (b) Non-successive failure analysis

3.3.3 Key block analysis

A detailed key block analysis was conducted using RocSlope3, with particular attention given to a structurally complex failure block identified during the successive failure simulation. The results are illustrated in Figure 14, where the slope is contoured by failure iteration, and the critical key block is distinctly highlighted in yellow. The visual output effectively demonstrates the progressive sequence of failure, showing how initial block removals lead to loss of confinement and the development of cascading instability through the slope mass. The highlighted key block was identified early in the failure sequence and played a pivotal role in initiating progressive failure. It is geometrically complex, defined by six intersecting planar joint surfaces, each contributing to the formation of a finite, removable block fully bounded in three dimensions.

This configuration satisfies the geometric criteria for key block formation under structurally controlled failure conditions and presents a high likelihood of instability when kinematic release surfaces are favourably oriented.

The detailed block information extracted from RocSlope3 also indicates that the highlighted key block failed primarily by sliding, with movement occurring along Joint 2 (bedding plane), which acted as the dominant release surface. The calculated FoS for this block was 0.908, placing it just below the critical stability threshold of 1.0 used in the analysis. This marginally unstable condition, coupled with the block's orientation and structural context, resulted in its early failure during the simulation. The block is situated along the mid-to-upper section of the batter face and aligns closely with the orientation of the bedding and intersecting joint sets. Its volume, while moderate (~30 m^3), is geometrically significant due to its complex configuration bounded by six distinct planar joint faces which fully define the block and contribute to its detachment. The spatial arrangement of these planes created a structurally interlocked geometry that, once released, not only triggered its own failure but also contributed to the progressive destabilisation of surrounding blocks by reducing confinement and exposing new release surfaces.

The iterative simulation results show that blocks such as this, once released, unlock new failure paths for surrounding material. This behaviour was not observed in the non-successive failure analysis, where block interactions are not recalculated after each failure event. Consequently, the successive failure model predicted a larger volume of failed material and a more extensive failure zone closely aligning with field observations of the actual slope failure.

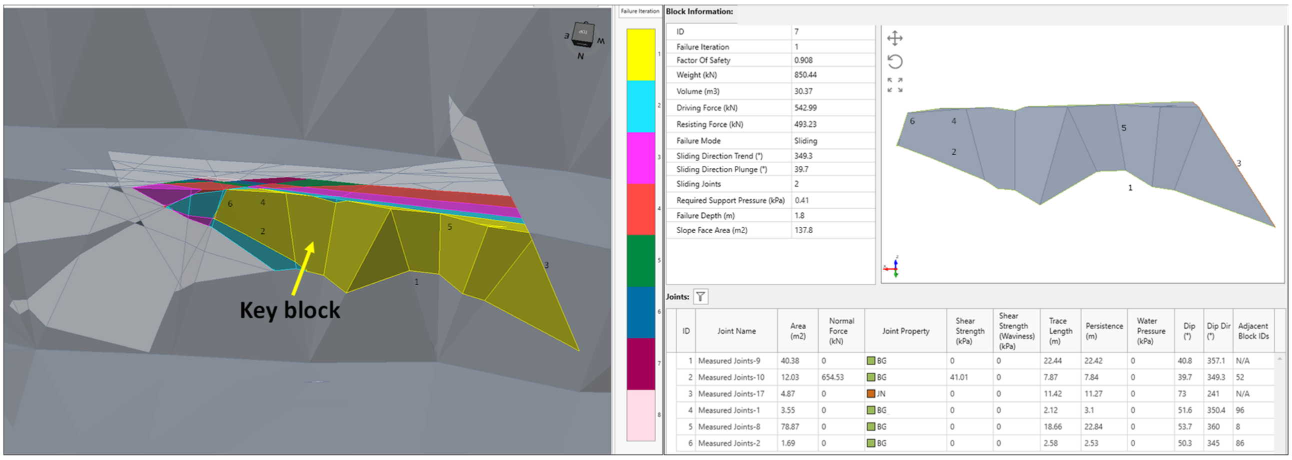

Figure 14 Key block analysis results from RocSlope3 with slope contoured by failure iteration and detailed block information

4 Future works and recommendations

The application of RocSlope3 in this study has proven effective for modelling structurally controlled slope failures and evaluating the influence of structural discontinuities on overall slope stability. However, the analysis has also highlighted key geotechnical and operational challenges at the study site that warrant further investigation and practical consideration in future slope design strategies. One of the most significant observations is the consistently low conformance to design geometry across the study area. In practice, the as-built slopes deviate from the intended pit design, with crest positions frequently laid back, resulting in shallower batter angles and narrow catch benches. As such, the achievable slope geometry is strongly influenced by the structural fabric of the rock mass, particularly where persistent discontinuities daylight into the pit face.

The comparison of successive failure simulations between the as-designed slope (batter angle of 65°) and the as-built slope (batter angle ~47°) demonstrates that pulling back the batter to align more closely with the mean bedding dip (~47°) can substantially reduce the severity and volume of failed material. This effectively increases the FoS by decreasing the driving forces associated with steep face angles and reducing the likelihood of key block formation along unfavourably oriented joints. The successive failure analysis confirms that slopes following the natural structural orientation are less prone to cascading block failures, thereby supporting the operational practice of laying back batters in structurally unfavourable zones. Based on these insights, future slope design in structurally complex zones should consider incorporating structural conformance into the design criteria, rather than relying solely on geometric targets such as uniform batter angles and bench widths. Where feasible, dip slope mining methods should be adopted in certain areas ensuring batter geometry aligned with dominant structural planes, particularly persistent bedding or joint sets, to reduce the potential for planar and wedge failures and improve slope reliability.

Additionally, future work should focus on improving the integration between geotechnical modelling and field execution. This includes higher-resolution structural mapping, possibly using photogrammetry, to refine input data for RocSlope3, and continuous feedback loops between model predictions and observed slope performance. These measures would support more adaptable, data-informed pit slope designs that balance geotechnical stability with mine productivity. In conclusion, the findings of this study support a shift toward structure-responsive slope design, especially in low-conformance areas where achieving the original pit geometry is unrealistic due to geological constraints. The use of RocSlope3's successive failure modelling, in conjunction with ongoing structural characterisation, offers a reliable framework for identifying failure-prone blocks and optimising batter geometries in line with the in situ structural regime.

5 Conclusion

This study underscores the complex interplay between slope geometry, structural discontinuities, and failure mechanisms in open pit slope design. The analysis clearly demonstrates that batter angle and discontinuity orientation are critical controls on slope stability, particularly in structurally controlled rock masses. The comparative analysis between original pit design and as-built geometries reveals that steeper batter angles (e.g. 65°) significantly increase the volume of failed material compared to flatter as-built slopes (47°), especially when the discontinuity dip approximates the batter angle. This highlights the increased risk of daylighting and planar or wedge failures under over steepened conditions. The application of RocSlope3's 3D block modelling with successive failure analysis also provided a realistic representation of failure progression, capturing block removability and cumulative failure volumes that closely aligned with field observations. The reliability of this approach is further validated by the match between modelled and actual failed volumes, confirming the utility of successive analysis for predictive geotechnical assessments. Moreover, the detailed key block analysis revealed that complex failure blocks often consist of multiple joint surfaces, with sliding typically occurring along critical planes such as Joint 2 in the observed key block, resulting in a FoS below 1.0. The ability to generate and analyse such block-specific failure data enhances the diagnostic power of slope stability assessments.

Importantly, while scaling the batter face to match the mean dip of bedding planes has been shown to reduce the number of daylighting surfaces and potential failures by up to 53.3%, this operational practice does not entirely eliminate failure risks. The occurrence of failure even after scaling reinforces the need for additional optimising batter geometries and geotechnical controls. Furthermore, laying back the crest to accommodate scaled batter angles often compromises berm capacity and catchment functionality, which must be factored into slope design trade-offs. In conclusion, this study affirms that integrating site-specific structural geology early in the design phase, coupled with advanced 3D block modelling and progressive failure analysis, provides a more reliable and robust framework for understanding and managing slope stability. These insights are essential for optimising pit wall performance, improving safety outcomes, and enhancing the predictability of failure behaviour in structurally controlled rock masses.

Acknowledgement

The authors acknowledge Rio Tinto Iron Ore for permission to publish this paper.

References

Bekele, A & Meten, M 2023, 'Modeling rock slope stability using kinematic, limit equilibrium and finite-element methods along Mertule Maryam–Mekane Selam road, central Ethiopia', *Modeling Earth Systems and Environment*, vol. 9, no. 2, pp. 1559–1585.

Bonilla-Sierra, V, Elmouttie, M, Donzé, FV & Scholtes, L 2017, 'Composite wedge failure using photogrammetric measurements and DFN-DEM modelling', *Journal of Rock Mechanics and Geotechnical Engineering*, vol. 9, no. 1, pp. 41–53.

Dixon, RA, Johnson, TM, de Graaf, PJH, Wessels, SDN & Venter, J 2011, 'Risk based geotechnical slope reconciliation at Rio Tinto Iron Ore, Pilbara Operations', *Proceedings of the 2011 International Symposium on Rock Slope Stability in Open Pit Mining and Civil Engineering*, Canadian Rock Mechanics Association, Alexandria.

Goldstein, D, Pace, R, Jung, JD, Young, D & Le Roux, KA 2023, 'Framework to predict open pit mine failure runout', in PM Dight (ed.), *SSIM 2023: Third International Slope Stability in Mining Conference*, Australian Centre for Geomechanics, Perth, pp. 629–638, https://doi.org/10.36487/ACG_repo/2335_41

Khanna, R & Dubey, RK 2021, 'Comparative assessment of slope stability along road-cuts through rock slope classification systems in Kullu Himalayas, Himachal Pradesh, India', *Bulletin of Engineering Geology and the Environment*, vol. 80, no. 2, pp. 993–1017.

Mensah, EK, Hammah, R, Basahel, H & Mitri, H 2025, 'Discrete fracture network application to rock slope engineering', *Journal of Industrial Safety*, vol. 2, no. 1, pp. 47–64.

Pradhan, SP & Siddique, T 2020, 'Stability assessment of landslide-prone road cut rock slopes in Himalayan terrain: a finite element method based approach', *Journal of Rock Mechanics and Geotechnical Engineering*, vol. 12, no. 1, pp. 59–73.

Rocscience Inc 2004, *Dips – Graphical and Statistical Analysis Software for Orientation Data*, version 8.029, computer software, Toronto, https://www.rocscience.com/software/dips

Rocscience Inc 2023, *RocSlope3 – 3D Block Stability Risk Assessment Software for Rock Slopes*, version 1.007, computer software, Toronto, https://www.rocscience.com/software/rocslope3

Sun, J, Ning, Y & Zhao, Z 2011, 'Comparative study of Sarma's method and the discontinuous deformation analysis for rock slope stability analysis', *Geomechanics and Geoengineering*, vol. 6, no. 4, pp. 293–302.

Trendall, AF & Blockley, J G 1970, 'The iron formations of the Precambrian Hamersley Group, Western Australia', *Geological Survey of Western Australia Bulletin*, vol. 119, pp. 365.